INSTITUTE OF PHYSICS PUBLISHING COMBUSTION THEORY AND MODELLING

Combust. Theory Modelling **6** (2002) 425–437 PII: S1364-7830(02)30001-9

Higher-order conditional moment closure modelling of local extinction and reignition in turbulent combustion

Chong M Cha[1] **and Heinz Pitsch**

Center for Turbulence Research, Stanford University, Stanford, CA 94305-3030, USA

E-mail: chongcha@stanford.edu

Received 23 October 2001, in final form 25 April 2002
Published 15 July 2002
Online at stacks.iop.org/CTM/6/425

Abstract

Higher-order, conditional moment closure approaches to modelling local extinction and reignition in turbulent, non-premixed combustion are investigated. This is done by studying closure strategies of the conditional source term itself. Feasibility studies are done using direct numerical simulation (DNS) experiments which exhibit varying degrees of local extinction. The higher-order conditional moments are taken directly from the DNS experiments as opposed to solving modelled transport equations for them. Results show that with moderate levels of extinction, the conditional probability density function (pdf) of the reduced temperature is unimodal, but skewed, and at least third-order terms in a series expansion of the nonlinear chemical source term conditional on the mixture fraction are required to predict the conditional means. With higher levels of local extinction, the conditional pdf shapes can be bimodal and third-order closure breaks down. The success of a presumed beta pdf shape for conserved scalars is well known. A beta probability distribution for the conditional reactive scalar cannot describe either the unimodal or bimodal pdf shapes which result from the local extinction and reignition events. However, predictions of the conditional means are excellent with the beta pdf model incorporated into a conditional moment closure modelling framework. The modelling results show little sensitivity to the conditional variances.

1. Introduction

Currently, a fundamental closure approximation in conditional moment closure modelling (Klimenko and Bilger 1999) of turbulent, non-premixed combustion is first-order closure of the average nonlinear chemical source terms, $\dot{\boldsymbol{w}}$, conditioned on the mixture fraction, $\xi(t, \boldsymbol{x})$:

$$\langle \dot{\boldsymbol{w}}(\boldsymbol{Y}(t, \boldsymbol{x}), \theta(t, \boldsymbol{x}), \rho(t, \boldsymbol{x}))|\xi(t, \boldsymbol{x}) = \eta\rangle \approx \dot{\boldsymbol{w}}(\langle \boldsymbol{Y}|\eta\rangle, \langle\theta|\eta\rangle, \langle\rho|\eta\rangle) \quad , \tag{1}$$

[1] Author to whom correspondence should be addressed.

1364-7830/02/030425+13$30.00

where $\boldsymbol{Y}$ is the vector of mass fractions of the reacting species, ρ is the density of the mixture, and η is the sample space variable of ξ. $\theta \equiv (T - T_\infty)/(T_\mathrm{f} - T_\infty)$ is the reduced temperature, where T_f is the complete conversion temperature and T_∞ is the reference temperature. The utility of first-order closure using conditional averaging is illustrated in figure 1, which shows in subplot (a) the reduced temperature θ as a function of ξ from the direct numerical simulation (DNS) experiment of Sripakagorn *et al* (2000). Subplot (b) shows the probability density function (pdf) of θ with the condition that ξ is within a given range of $\xi_\mathrm{st} \pm \Delta\eta$, where ξ_st is the stoichiometric value of the mixture fraction, 0.5 for this case. $\Delta\eta$ decreases from the dash–dotted line to the dashed line and finally to $\Delta\eta \approx 0$ for the solid line. Thus, the solid line is a representation of the conditional pdf of θ at $\xi = \xi_\mathrm{st}$. The figure illustrates three points: (a) the inapplicability of first-moment closure under conventional (unconditional) averaging, as is well known; (b) the much improved representation of the pdf of θ by its mean value alone due to conditioning on ξ, helping to validate (1); and (c) a negative skewness of the pdf due to the existence of local extinction and reignition events in this experiment, which threatens the validity of (1). The extinction/reignition events, clearly visible in subplot (a) and evident in the pdfs at low values of θ_st in subplot (b), are interpreted as fluctuations about the conditional mean in a conditional moment closure modelling framework.

Recently, modelling of the conditional variance has been proposed to improve closure of the conditional chemical source term: the conditional variance can be used (a) in an additional, second-order correction to (1) (Kronenburg *et al* 1998, Mastorakos and Bilger 1998, Swaminathan and Bilger 1998), or (b) to construct a presumed pdf shape of one or more reactive scalars (Klimenko and Bilger 1999). Presently, we investigate the feasibility of both these higher-order, conditional moment closure approaches for local extinction/reignition modelling by quantifying the differences between using truncated series expansions and an integral over a conditional pdf for the reaction rate. The DNS experiment of Sripakagorn

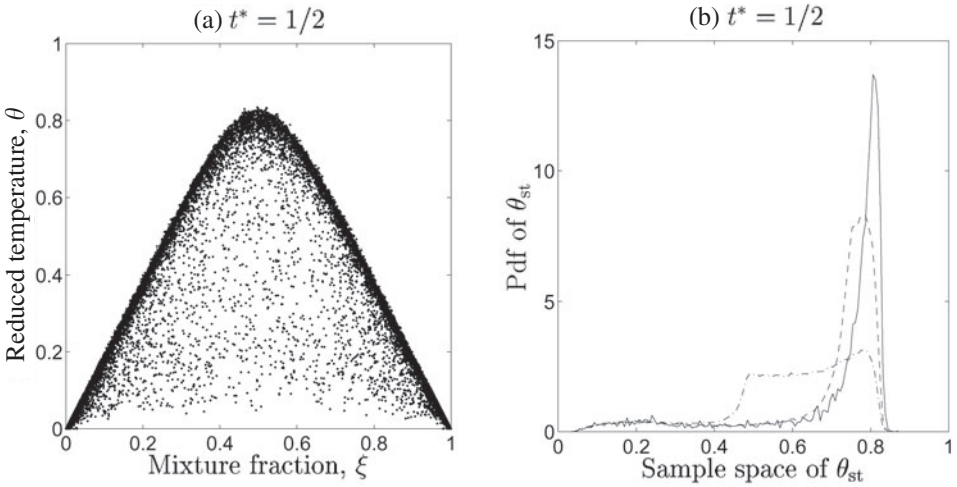

Figure 1. Motivation of the work. Subplot (*a*) is a scatter plot of the reduced temperature, θ, as a function of the local mixture fraction, ξ, at $t^* = 1/2$ (time has been non-dimensionalized by the initial large-eddy turnover time) from the 128^3 DNS experiment of Sripakagorn *et al* (2000). (The DNS is described in section 2 of this paper.) Subplot (*b*) shows the conditional pdf of θ conditioned on ξ within a decreasing range, $\pm\Delta\eta$, of ξ values about $\xi_\mathrm{st} = 0.5$, the stoichiometric value of the mixture fraction. The range decreases from the dash–dotted line ($\Delta\eta = 0.25$), to the dashed line ($\Delta\eta = 0.1$), and finally to $\Delta\eta = 0.005$.

et al (2000), specifically designed to investigate extinction/reignition, offers an ideal test-case to investigate the merits and drawbacks of the higher-order conditional moment closure strategies. The modelling issues associated with closure of the conditional variance equations can be found in Swaminathan and Bilger (1998). Here, we use the exact conditional variance (and higher moments) available from the DNS to focus on the errors associated with the closure strategies for the conditional chemical source term rather than those associated with the modelling assumptions required to close the higher-order conditional moment equations.

The paper is organized as follows. In the next section, the DNS experiments used to test the modelling approaches are reviewed. In section 3, the higher-order closure strategies are described and the governing equations are given. In section 4, *a priori* modelling comparisons are made with the DNS experiments of a one-step, second-order, reversible global reaction in homogeneous, isotropic, and decaying turbulence. Finally, the paper concludes with an assessment of the two conditional moment closure modelling approaches for describing extinction/reignition.

2. DNS experiment

The production rates for fuel (F), oxidizer (O), and product (P) for the present numerical experiment of $\mathrm{F} + \mathrm{O} \xrightarrow[k/K]{k} 2\mathrm{P}$ evolving in isotropic, homogeneous, and decaying turbulence are $\dot{w}_\mathrm{F} = -\dot{w}$, $\dot{w}_\mathrm{O} = -\dot{w}$, and $\dot{w}_\mathrm{P} = 2\dot{w}$, respectively, where

$$\dot{w}(Y_\mathrm{F}, Y_\mathrm{O}, Y_\mathrm{P}, \theta) = kY_\mathrm{F}Y_\mathrm{O} - \frac{k}{K}Y_\mathrm{P}^2 \tag{2}$$

$$k(\theta) \equiv A \exp\left(-\frac{\mathrm{Ze}}{\alpha}\right) \exp\left[-\frac{\mathrm{Ze}(1-\theta)}{1-\alpha(1-\theta)}\right].$$

Here, A is the frequency factor (multiplied by density and divided by molecular weight, assumed equal for all species), $\alpha \equiv (T_\mathrm{f} - T_\infty)/T_\mathrm{f}$ is the heat release parameter, and $\mathrm{Ze} \equiv \alpha T_\mathrm{a}/T_\mathrm{f}$ is the Zeldovich number. T_a is the activation temperature. T_f is defined for the one-step, irreversible chemistry scheme, i.e. for $K = \infty$ or no backward reaction. For the above reversible chemistry scheme, with finite K, the maximum value of θ, denoted by θ_eq, is less than unity. The 'equilibrium constant' is held fixed at $K = 100$ to help insure the resolution of the reaction zone in the numerics. With $K = 100$, the resulting maximum value of $\theta_\mathrm{eq} = 0.83$ at ξ_st. The Schmidt number is 0.7 and Lewis numbers are unity. The turbulent flow is governed by the incompressible Navier–Stokes equations with viscosity independent of the temperature (cf Sripakagorn *et al* (2000) for details of the simulation).

Chemistry rate parameters in (2) are $\alpha = 0.87$ and $\mathrm{Ze} = 4$. Values of A define different numerical experiments with low ($A = 13.0 \times 10^4$), moderate ($A = 8.0 \times 10^4$), and high ($A = 0.3 \times 10^4$) levels of local extinction. These cases correspond to 'Case A', 'Case B', and 'Case C', respectively. Categorization of the level of local extinction by the terms 'low', 'moderate', and 'high' are described later in this paper. These experimental cases were used to investigate local extinction/reignition in another extension of conditional moment closure modelling (Cha *et al* 2001). The present, singly conditional moment closure modelling extensions are to be distinguished from this previous investigation of a doubly conditional moment closure approach. In Cha *et al* (2001), the modelling focused on improving first-moment closure for the extinction/reignition problem by introducing a second conditioning variable, the scalar dissipation rate, $\chi \equiv 2\mathcal{D}(\nabla\xi)^2$, to account for the additional fluctuations about the singly conditional means not attributable to ξ. In the definition of χ, $\mathcal{D}$ is the molecular diffusivity of ξ. In all three numerical experiments, the evolution of the turbulent scalar dissipation rate field is identical. The A values in the chemical source term of the species

transport equations are changed to alter the quenching value of χ to, in effect, yield the varying levels of the conditional fluctuations of θ (cf Cha *et al* (2001) for details). Cha *et al* (2001) discuss the influence of the fluctuations of χ on the θ fluctuations. We review some results from this work later in this paper. Here, the focus is on the impact of these θ fluctuations on singly conditional closure strategies of the chemical source term.

3. Conditional moment closure approaches

3.1. Higher-moment conditional moment closure approaches

The conditioned average of $\dot{w}$ as a function of all conditional moments can be obtained with: (a) a series expansion of the exponential in (2) about $\langle\theta|\eta\rangle \equiv \theta - \theta'$ with $\epsilon \equiv \alpha\theta'/(1-\alpha(1-\langle\theta|\eta\rangle))$, valid for $|\epsilon| < \infty$; (b) a series expansion for $(1+\epsilon)^{-1}$, valid for $|\epsilon| < 1$; and (c) a decomposition of all species mass fractions about their conditional means, $Y \equiv \langle Y|\eta\rangle + Y'$, where Y' represents the fluctuation about the conditional mean. Conditionally averaging, the result yields

$$\langle\dot{w}(Y_\mathrm{F}, Y_\mathrm{O}, Y_\mathrm{P}, \theta)|\eta\rangle = \dot{w}(\langle Y_\mathrm{F}|\eta\rangle, \langle Y_\mathrm{O}|\eta\rangle, \langle Y_\mathrm{P}|\eta\rangle, \langle\theta|\eta\rangle)(1+\mathcal{B}+\mathcal{C}+\cdots), \tag{3}$$

where

$$\mathcal{B} = \frac{\langle Y'_\mathrm{F}Y'_\mathrm{O}|\eta\rangle}{\langle Y_\mathrm{F}|\eta\rangle\langle Y_\mathrm{O}|\eta\rangle} - \frac{1}{K}\frac{\langle Y'^2_\mathrm{P}|\eta\rangle}{\langle Y_\mathrm{P}|\eta\rangle^2} + \frac{\mathrm{Ze}}{[1-\alpha(1-\langle\theta|\eta\rangle)]^2}\left(\frac{\langle Y'_\mathrm{F}\theta'|\eta\rangle}{\langle Y_\mathrm{F}|\eta\rangle}\right.$$
$$\left. + \frac{\langle Y'_\mathrm{O}\theta'|\eta\rangle}{\langle Y_\mathrm{O}|\eta\rangle} - \frac{2}{K}\frac{\langle Y'_\mathrm{P}\theta'|\eta\rangle}{\langle Y_\mathrm{P}|\eta\rangle}\right) + \left(\frac{\mathrm{Ze}/2}{1-\alpha(1-\langle\theta|\eta\rangle)} - \alpha\right)\frac{\langle\theta'^2|\eta\rangle(1-1/K)}{[1-\alpha(1-\langle\theta|\eta\rangle)]^3}$$

$$\mathcal{C} = \left(\frac{\mathrm{Ze}/2}{1-\alpha(1-\langle\theta|\eta\rangle)} - \alpha\right)\frac{\alpha^2/\mathrm{Ze}}{1-\alpha(1-\langle\theta|\eta\rangle)}\left(\frac{\langle Y'_\mathrm{F}\theta'^2|\eta\rangle}{\langle Y_\mathrm{F}|\eta\rangle} + \frac{\langle Y'_\mathrm{O}\theta'^2|\eta\rangle}{\langle Y_\mathrm{O}|\eta\rangle} + \frac{2}{K}\frac{\langle Y'_\mathrm{P}\theta'^2|\eta\rangle}{\langle Y_\mathrm{P}|\eta\rangle}\right)$$
$$+ \frac{\alpha}{1-\alpha(1-\langle\theta|\eta\rangle)}\left(\frac{\langle Y'_\mathrm{F}Y'_\mathrm{O}\theta'|\eta\rangle}{\langle Y_\mathrm{F}|\eta\rangle\langle Y_\mathrm{O}|\eta\rangle} - \frac{1}{K}\frac{\langle Y'^2_\mathrm{P}\theta'|\eta\rangle}{\langle Y_\mathrm{P}|\eta\rangle^2}\right)$$
$$- \frac{\alpha^4/\mathrm{Ze}}{[1-\alpha(1-\langle\theta|\eta\rangle)]^2}\langle\theta'^3|\eta\rangle\left(1-\frac{1}{K}\right)$$

valid for $|\epsilon| < 1$. The complete series is always convergent for $\alpha \leqslant 1$.

For the present case of a single-step reaction, the conditional averages of all species and temperature can be obtained from the single equation for the average of θ conditioned on ξ

$$\left(\frac{\mathrm{d}}{\mathrm{d}t} - \frac{\langle\chi|\eta\rangle}{2}\frac{\partial^2}{\partial\eta^2}\right)\langle\theta|\eta\rangle = 2\dot{w}(\langle Y_\mathrm{F}|\eta\rangle, \langle Y_\mathrm{O}|\eta\rangle, \langle Y_\mathrm{P}|\eta\rangle, \langle\theta|\eta\rangle)(1+\mathcal{B}+\mathcal{C}). \tag{4}$$

$\langle\chi|\eta\rangle$ is the conditionally averaged dissipation rate of ξ, specified directly from the DNS. e_Q and e_Y closure has been invoked (Cha *et al* 2001). For convenience, (4) is referred to as the `cmc3` model (third-order closure), as the `cmc2a` model with $\mathcal{C} = 0$ (second-order closure), and as the `cmc1` model with both $\mathcal{B} = 0$ and $\mathcal{C} = 0$ (first-order closure). All double and triple conditional correlations are taken from the DNS.

3.2. Presumed conditional pdf approach

The beta distribution, or 'beta pdf', is a standard model to describe a random variable, $\boldsymbol{\Theta}$ say, whose set of all possible values lies is some finite interval $[\Theta^-, \Theta^+]$ (Ross 1984). The beta pdf is a two parameter distribution given by

$$p_\Theta(\Theta) = \frac{1}{B(a,b)}(\Theta-\Theta^-)^{a-1}(\Theta^+-\Theta)^{b-1}(\Theta^+-\Theta^-)^{1-a-b} \tag{5}$$

for $\Theta^- < \Theta < \Theta^+$, where Θ is the sample space variable of $\boldsymbol{\Theta}$. The free parameters a and b enforce the first and second moments of $\boldsymbol{\Theta}$ and are given by

$$a = \frac{\langle\boldsymbol{\Theta}\rangle - \Theta^-}{\Theta^+ - \Theta^-}\left(\frac{(\langle\boldsymbol{\Theta}\rangle - \Theta^-)(\Theta^+ - \langle\boldsymbol{\Theta}\rangle)}{\langle\boldsymbol{\Theta}'^2\rangle} - 1\right),$$
$$b = \frac{\Theta^+ - \langle\boldsymbol{\Theta}\rangle}{\langle\boldsymbol{\Theta}\rangle - \Theta^-}a \ ,$$

where $\langle\boldsymbol{\Theta}\rangle$ and $\langle\boldsymbol{\Theta}'^2\rangle$ are the mean and variance of $\boldsymbol{\Theta}$, respectively. It is sometimes useful to write the pdf in (5) as '$p_{\boldsymbol{\Theta}}(\Theta; a, b)$', explicitly showing this parametrization, or further, as '$p_{\boldsymbol{\Theta}}(\Theta; t, \boldsymbol{x})$', if $a(t, \boldsymbol{x})$ and $b(t, \boldsymbol{x})$ varied in time and space, for example. Both notations equivalently represent '$p_{\boldsymbol{\Theta}}(\Theta)$' in (5). In (5), $B(a, b)$ normalizes the pdf such that $\int p_{\boldsymbol{\Theta}}(\Theta)\,\mathrm{d}\Theta = 1$.

The presumed beta pdf model for describing the mixing of a conserved scalar is described in Bilger (1980). For the present case of a single-step reaction, $p_{\boldsymbol{\Theta}}(\Theta)$ models the conditional pdf of the reacting scalar θ on ξ, written as $p_{\theta|\xi}(\Theta)$. θ is bound by $0 \leqslant \theta \leqslant \theta_{\mathrm{eq}}(\eta)$, where θ_{eq} is the equilibrium profile, a function of the mixture fraction. (This function is known ahead of time from a given chemical kinetic model.) That is, $\Theta^- = 0$ and $\Theta^+ = \theta_{\mathrm{eq}}$ for any given value of $\xi = \eta$. Applying the presumed beta pdf $p_{\theta|\xi}(\Theta)$ to the conditional moment closure equations yields

$$\left(\frac{\mathrm{d}}{\mathrm{d}t} - \frac{\langle\chi|\eta\rangle}{2}\frac{\partial^2}{\partial\eta^2}\right)\langle\theta|\eta\rangle = 2\int \dot{w}(Y_{\mathrm{F}}, Y_{\mathrm{O}}, Y_{\mathrm{P}}, \theta)\,p_{\theta|\xi}(\Theta)\,\mathrm{d}\Theta \ , \tag{6}$$

where $\dot{w}(Y_{\mathrm{F}}, Y_{\mathrm{O}}, Y_{\mathrm{P}}, \theta)$ is a known function of the ξ and θ sample space and $p_{\theta|\xi}(\Theta)$ is parametrized by the conditional mean and variance of θ, $\langle\theta|\eta\rangle$ and $\langle\theta'^2|\eta\rangle$, respectively, through $a(t, \eta)$ and $b(t, \eta)$ (see below). Equation (6) is an integro-differential equation for $\langle\theta|\eta\rangle(t, \eta)$ and only $\langle\theta'^2|\eta\rangle$ is taken from the DNS to evaluate the right-hand side of (6) for the *a priori* study. Equation (6) is referred to as the `cmc2b` model throughout the remainder of the paper.

3.3. Implementation issues

Conditionally averaged quantities from the DNS required for the *a priori* modelling studies include $\langle\chi|\eta\rangle(t, \eta)$, $\langle\theta^2|\eta\rangle(t, \eta)$, and $\langle\theta|\eta\rangle(0, \eta)$ for all the higher-order conditional moment closure approaches. $\langle\theta^3|\eta\rangle(t, \eta)$ is also required for the `cmc3` model.

The conditionally averaged scalar dissipation rate can be decomposed as $\langle\chi|\eta\rangle = \langle\chi|\xi_{\mathrm{st}}\rangle \exp\{-2[\mathrm{erf}^{-1}(2\eta - 1)]^2\}$ (Cha *et al* 2001) with no appreciable effect on the solutions.

Binning of the DNS experimental data in η is done with equal points per bin as opposed to using equally incremented bin sizes for calculating all conditional means, resulting in more accurate and smoother profiles. Because there is an equal amount of fuel and oxidizer in the system, as mixing proceeds, the number of data points increases with time towards $\xi = 0.5 = \xi_{\mathrm{st}}$. With the above binning procedure then, the bin width at ξ_{st} decreases with increasing time. In figure 1(*a*) for example, which shows less than 1% of the total available 128^3 DNS data points (randomly chosen), $\Delta\eta = 0.02$ at ξ_{st} with 128 bins; at a later time, $t^* = 1$, $\Delta\eta = 0.01$ at ξ_{st}. For a given ξ bin then, there is always a constant number of data points, of the order of 10^4. The accuracy of an ensemble is proportional to the inverse of the square root of the number of points. This yields an uncertainty of about $\pm 0.8\%$ for a singly conditional mean; double and triple this value for second- and third-order statistics, respectively. The uncertainties add for each product and divide in the calculations for $\mathcal{B}$ and $\mathcal{C}$ in (4). Thus, for example, the uncertainty in $\mathcal{C}$ would be of the order of 5%. The `cmc3` model results show no appreciable change within these and higher uncertainties: it takes $\pm 30\%$ relative errors added

to the DNS second- and third-order statistics to yield a 5% maximum difference in the $\langle\theta|\eta\rangle$ modelling results. Cubic interpolation is used in ξ space to interpolate all the one-dimensional profiles onto a fixed η grid. Cubic splines are used to interpolate the required one-dimensional profiles in time where the DNS data are not available. (Note, DNS data are always available within the ξ_{st} bin, as discussed above.) Boundary conditions for equations (4) and (6) at $\eta = 0, 1$ are $\langle\theta|\eta\rangle(t, 0) = \langle\theta|\eta\rangle(t, 1) = 0$.

For the `cmc2b` model, the conditional pdf on the right-hand side of (6) can be written as

$$p_{\theta|\xi}(\Theta; t, \eta) = \frac{\Gamma(a+b)}{\Gamma(a)\Gamma(b)}\Theta^{a-1}(\theta_{eq} - \Theta)^{b-1}\theta_{eq}^{1-a-b}.$$

Here, Γ is the gamma function (Press *et al* 1992), and

$$a(t, \eta) = \frac{\langle\theta|\eta\rangle}{\theta_{eq}}\left(\frac{\langle\theta|\eta\rangle(\theta_{eq} - \langle\theta|\eta\rangle)}{\langle\theta'^2|\eta\rangle} - 1\right)$$

$$b(t, \eta) = \frac{\theta_{eq} - \langle\theta|\eta\rangle}{\langle\theta|\eta\rangle}a$$

where the (t, η) dependences come through relating a and b to $\langle\theta|\eta\rangle$ and $\langle\theta'^2|\eta\rangle$. For the present Arrhenius reaction rate (Ze = 4), the source term is sufficiently localized about ξ_{st} in mixture fraction space and θ_{eq} can be set to θ_{eq} at ξ_{st} for all η with no appreciable effect on the solutions. (For the present, one-step reversible reaction with $K = 100$, this value is $\theta_{eq} = 0.83$.) This approximation would become even more accurate with increasing Ze. The beta pdf can be zero or infinity at or near the Θ boundaries. Trapezoidal integration is used for the right-hand side of (6), with the contributions near the boundaries given by $0.5(\Theta_N - \Theta_{N-1})\dot{w}_{N-1}(\Theta)$ at the $\Theta_{N-1/2}$ grid point and an analogous contribution at $\Theta_{1/2}$.

4. Results and discussion

Figure 2 compares the higher-moment modelling results (lines) to the DNS experimental data (symbols). Solid circles are the conditionally averaged temperatures at ξ_{st} taken directly from the experiment. Subplot (*a*) is from the same case as was shown in figure 1. The deviation of $\langle\theta|\xi_{st}\rangle$ from the equilibrium value, $\theta_{eq} = 0.83$ at ξ_{st}, is due to the local extinction/reignition events that were seen in figure 1(*a*). Only the frequency factor was decreased in the DNS for the case shown in figure 2(*b*), which results in increased extinction levels, and hence shows a larger deviation from θ_{eq} as compared to the case in subplot (*a*). Open circles are the standard deviation about $\langle\theta|\xi_{st}\rangle$ and open triangles are the (non-dimensional) skewness defined as

$$s = \frac{1}{\langle\theta'^2|\eta\rangle^{3/2}}\int(\Theta - \langle\theta|\eta\rangle)^3 p_{\theta|\xi}(\Theta)\,\mathrm{d}\Theta,$$

where $p_{\theta|\xi}(\Theta)$ is the conditional pdf. Note that s is a function of $\langle\theta^3|\eta\rangle$, a third-order term. Hence, only the `cmc3` model explicitly incorporates the skewness. In figure 2, solid lines are first-order modelling results (`cmc1`), dashed lines are second-order predictions (`cmc2a`), and dash–dotted lines are third-order modelling results (`cmc3`).

Cha *et al* (2001) discuss the limitations of `cmc1` modelling of local extinction and reignition. To summarize, local extinction events cannot be accounted for by `cmc1` modelling and thus the DNS data are overpredicted for case B (subplot (*a*) in figure 2). A reignition mechanism does not exist in `cmc1` modelling and thus first-moment closure predicts global extinction for case C, although the DNS data recover to a burning state (subplot (*b*) in figure 2). (Deviations of `cmc1` modelling predictions from the DNS data for case A were small, as extinction levels for this case are low.) Presently, we are interested in the extent the higher-moment closure strategy can correct for the shortcomings of `cmc1` modelling.

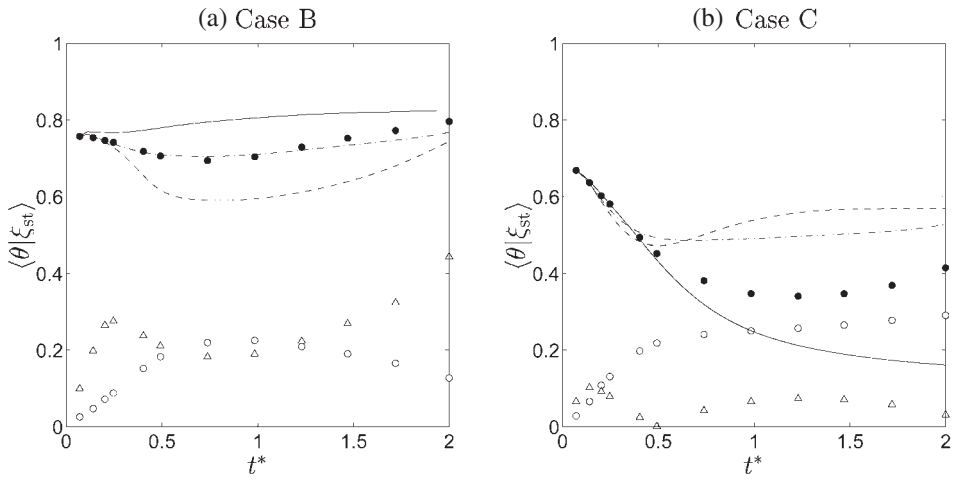

Figure 2. Comparison of higher-moment modelling results with DNS data. ●, conditional average of the reduced temperature, $\langle\theta|\xi_{st}\rangle$; ○, standard deviation about conditional means, $(\langle\theta'^2|\xi_{st}\rangle)^{1/2}$; △, skewness, $|s|/10$. ——, first-order, conditional moment closure results (`cmc1`); - - - -, second-order modelling results (`cmc2a`), and — · —, third-order predictions (`cmc3`). Subplot (*a*) moderate extinction case (case B) and subplot (*b*) high extinction case (case C) from Cha *et al* (2001). The bin widths are of the order of 0.01; less than 0.01 for times $t^* > 1/2$ (cf discussion of section 3.3).

In case B (subplot (*a*) in figure 2), second-order closure causes the mean to be underpredicted. Consideration up to the third-order terms in (4) evidently counteracts this effect and leads to good predictions of the data. (The modelling results for case A (not shown) are similar to case B but with much smaller deviations from the data.)

In case C (subplot (*b*) in figure 2), first-order closure is unable to predict the onset of reignition (in the mean). Both second- and third-order closures can predict the global reignition, but deviate from the data beyond $t^* \gtrsim 1/2$. Of note is that the skewness, $|s|$, decreases in the higher extinction case while the variance remains comparable.

Discussion of the modelling results in figure 2 centre around the conditional pdfs of θ at ξ_{st} for representative times of interest. (case A is not discussed here, as extinction levels are low and do not significantly impact the conditional pdfs.) The left column of figure 3 shows $p_{\theta|\xi}$ at ξ_{st}, $t^* = 1/4, 1/2, 3/4$, and $3/2$ for case B. At early times ($t^* < 1/2$), the pdfs are unimodal—have a well-defined, single peak—with some negative skewness. The series expansion of the conditionally averaged reaction rate, (3), does not know the shape of the pdf. Evidently, skewness, or third-order information, and variance, or second-order information, are sufficient to correct first-moment closure, resulting in the good agreement with the data that was seen in figure 2(*a*). For larger times, $t^* \geqslant 1/2$, some bimodality begins to appear in the pdfs, but not enough to cause problems for third-order closure, the `cmc3` model. For a general unimodal pdf, at least third-order moments are required to capture skewness. For this experimental case with moderate local extinction levels, the skewness is always negative for $p_{\theta|\xi}$ as the temperature can never exceed θ_{eq}. The implication is that in such a circumstance at least third-order information is required in the series expansion of $\langle\dot{w}|\eta\rangle$.

The right column of figure 3 shows $p_{\theta|\xi}$ at ξ_{st} for case C (corresponding to subplot (*b*) in figure 2) at $t^* = 1/4, 1/2, 3/4$, and $3/2$. For $t^* \lesssim 1/4$, the standard deviation about the conditional average is comparable to case B, but with reduced skewness (cf figure 2), and second-order closure yields comparable results to the third-order closure predictions.

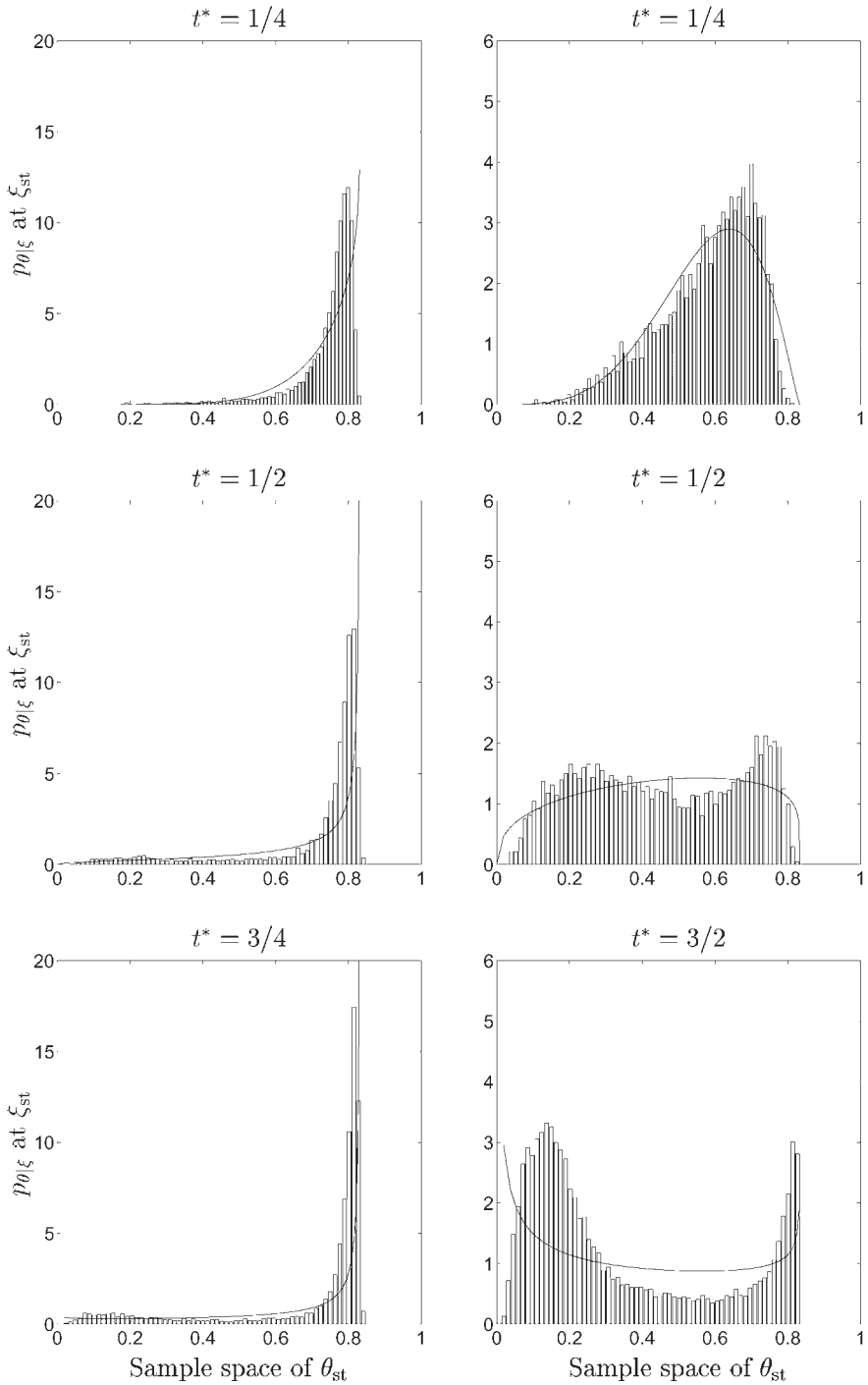

Figure 3. Conditional pdfs of θ at $\xi_{\rm st}$ for case B (left column) and case C (right column). Solid lines are the presumed beta pdf predictions using the exact conditional means and variances from the DNS. Approximately 10^4 data points are used to generate the pdfs (cf discussion of section 3.3).

For $t^* \gtrsim 1/2$, the pdfs become bimodal—have well-defined, double peaks—and thus the skewness can no longer characterize the shape of the pdfs. Third-order closure also breaks down. Bimodality becomes stronger for increasing times with comparable peak temperatures. The comparable standard deviations from the conditional mean for this case as compared to case B (cf figure 2) is due to the combined effect of the high extinction levels in this case, which decrease $\langle\theta|\xi_{\rm st}\rangle$, and the bimodality of the pdf. The cause of the reduction in the skewness from case B is due to the remarkable symmetry in the pdfs.

The skewed unimodal and bimodal pdf shapes in figure 3 are due to the realistic, Arrhenius kinetics which result in a bistable dynamic system (Pitsch and Fedotov 2001), as determined by the steady flamelet solution (Peters 1983). With low to moderate local extinction levels, the extinction events lead to the negatively skewed pdf shapes, as was seen in the left column of figure 3 (case B). With moderate to high extinction levels, the upper and lower stable branches lead to the bimodal pdf shapes, as was seen most dramatically in the right column of figure 3 (case C) for times $t^* > 1/2$. That the transitional probabilities always correspond to the minimum probability of the bimodal distributions is a direct result of the unsteady dynamics of the bistable system switching between the upper, high temperature ($\theta_{\rm st} \sim \mathcal{O}(1)$) and lower, low temperature ($\theta_{\rm st} \sim \mathcal{O}(0.1)$) stable branches (Pitsch *et al* submitted). This switching is of course due to extinction and reignition.

Figure 3 also shows the predictions of the conditional pdf shapes using the presumed beta pdf model (solid lines). In this figure, both the conditional mean and variance were taken directly from the DNS data. The success of the presumed beta pdf model for passive scalar mixing is well known. Figure 3 shows that the presumed beta pdf model does not have the flexibility to describe the variety of reactive scalar pdf shapes due to the modifications by reaction, more precisely, the extinction/reignition dynamics which result from realistic Arrhenius kinetics. In particular, the unimodal peaks are always underpredicted for case B (left column). In case C (right column), the presumed beta pdf shape also underpredicts the twin peak densities of the bimodal pdfs, while the transitional probabilities between the extinguished and burning states are always overpredicted.

In spite of the failure of the presumed beta pdf model to describe the unimodal and bimodal conditional pdf shapes of the reduced temperature, *a priori* modelling results of (6), the `cmc2b` model, show surprisingly excellent agreement with the DNS experiments. Figure 4 compares `cmc2b` modelling results for $\langle\theta|\xi_{\rm st}\rangle$ (solid lines) to the DNS experimental data (symbols). Model `cmc1`, first-moment closure results are given by the dashed lines. Only the conditional variance, $\langle\theta'^2|\xi\rangle$, is taken from the DNS to evaluate the right-hand side of (6) for the `cmc2b` modelling results. For all cases, `cmc2b` modelling yields improved predictions over first-moment closure. In particular, for case B, `cmc2b` modelling can accurately describe the effect of local extinction on the singly conditional means. For case C, `cmc2b` modelling accurately predicts the transition back to a burning state. We remind the reader that `cmc2a`, which also only uses the conditional variance, could not accurately predict this transition.

Discussion of the excellent agreement between `cmc2b` modelling results and the DNS data centre around the singly conditional pdfs of figure 3. The cancellation of errors between the presumed beta distribution and the actual reactive scalar pdfs (that were discussed in relation to figure 3) can be seen from equation (6). The right-hand side can be reinterpreted as the integral over the presumed beta pdf shape weighted by the nonlinear chemical source term. Figure 5 shows representative results reproduced from figure 3 with the chemical source term function (dashed lines) overlaid. The figure shows how the strong nonlinearity of the chemical source term cancels the errors made by the presumed beta distribution. When the pdf is unimodal (case B), the large underprediction of the peak value made by the presumed beta pdf model is diminished by the strongly vanishing chemical source term as $\theta_{\rm st} \to \theta_{\rm eq}$

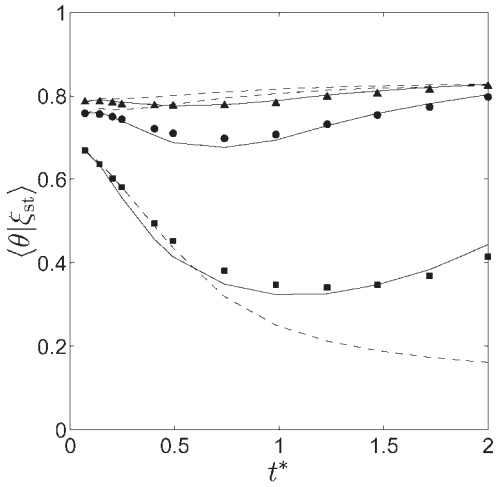

Figure 4. Comparison of presumed beta pdf modelling results (lines) with DNS data (symbols). Symbols are DNS data of the conditional average of the reduced temperature at stoichiometric, $\langle\theta|\xi_{\rm st}\rangle$: ▲, low extinction level case (case A); ●, moderate extinction level case (case B), and ■, high extinction level case (case C). ——, presumed beta pdf modelling results (`cmc2b`) and - - - -, first-order, conditional moment closure results (`cmc1`).

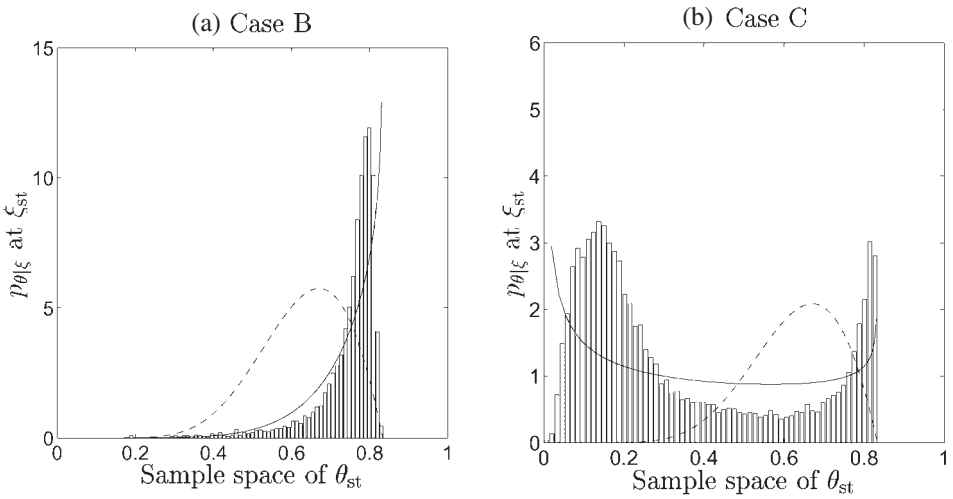

Figure 5. Why the presumed beta pdf modelling works. Representative results reproduced from figure 3 with the chemical source term function (- - - -) overlaid.

and offsets the overprediction made by the beta pdf at lower temperatures. When the pdf is bimodal (case C), only the transitional and high temperature probabilities are significant and a similar cancellation of errors occurs as in the unimodal case. The strong nonlinearity of the chemical source term, due to the realistic Arrhenius kinetic model, leads to a bistable system and the characteristic unimodal and bimodal pdf shapes already described. Ironically, figure 5 shows that it is the strong nonlinearity of the chemical source term which leads to

the cancellation of errors under cmc2b modelling. Hence, this type of cancellation of errors is also expected to occur in reacting flows of practical interest, where Arrhenius kinetics are used.

Figure 6 shows sensitivity results of cmc2b modelling to the conditional variance. Solid lines reproduce the results from figure 4, which use the exact variance from the DNS. Dashed lines show results with ±30% relative errors added to the DNS variance. The results show little sensitivity of the singly conditional means as predicted by cmc2b modelling to the actual DNS variances. Swaminathan and Bilger (1998) discuss the modelling issues associated with the conditional variance. The present sensitivity study, shown in figure 6, suggests that in practice even a crude estimate of the conditional variance may be sufficient to predict the effects of local extinction and reignition on $\langle\theta|\xi\rangle$.

The insensitivity of the cmc2b modelling to the conditional variance may not hold for larger Zeldovich numbers than the present value of Ze = 4. (Ze ≈ 8 for hydrocarbon combustion.) Increasing the Ze would shift the onset of the exponential rise in the chemical source term function to higher temperatures than seen in figure 5. Below this higher temperature, the errors between the actual and presumed beta pdf would then become unimportant as $\dot{w} = 0$ there (cf the previous discussion surrounding figure 5). However, the discrepencies at and near the upper peak values of the pdfs would be weighted more due also to the shift in the maximum value of $\dot{w}$ to higher temperatures with increasing Ze. This assumes that the general form of the conditional pdfs, as shown in figure 5 for example, are unaffected by a larger Ze. However, for larger Ze, the quenching value of the scalar dissipation rate will decrease. This will increase the timescale for the extinction events and hence increase the transitional probabilities relative to the upper peak value. This could improve the beta pdf representation of the conditional pdfs. The net impact of these competing effects cannot be presently gauged beyond this speculation and it is acknowledged that the sensitivity of cmc2b modelling to the conditional variance may be higher for larger Zeldovich numbers.

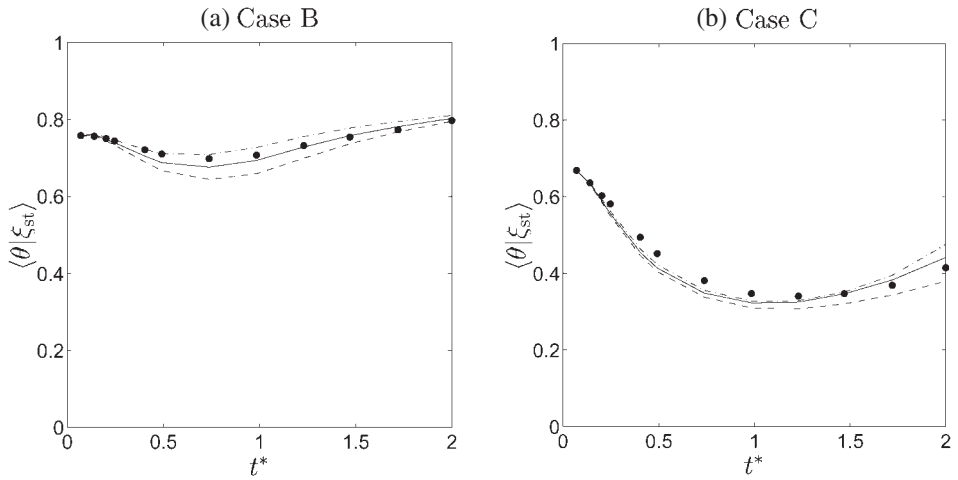

Figure 6. Sensitivity study of cmc2b modelling to conditional variance. Symbols, DNS data of singly conditional average of the reduced temperature at stoichiometric, $\langle\theta|\xi_{st}\rangle$ (●). Lines, cmc2b modelling results: exact variance, $\langle\theta'^2|\xi\rangle$, from DNS used in the *a priori* modelling results (——), ±30% relative errors added to the DNS variance (- - - -).

5. Conclusions

Higher-order strategies providing closure for the chemical source term in conditional moment closure modelling are investigated. Feasibility studies are carried out by using higher-order conditional statistics taken directly from direct numerical simulation experiments which exhibit local extinction and reignition. Modelling issues associated with closure of the transport equations for the higher-order moments are not addressed.

With moderate levels of local extinction, the conditional pdfs are unimodal (single peaked). Mean and variance information alone in the series expansion of the conditional average of the chemical source term is insufficient to describe the influence of the fluctuations. That is, first- and second-order closure cannot describe the conditional means and third-moments (or the skewness of the pdfs) are also required to obtain good predictions. With high levels of local extinction, the pdf can adopt a strong bimodal shape and third-order closure is insufficient to describe the conditional averages.

Conditional second moment information is only sufficient to describe the effect of extinction/reignition on the conditional averages if a presumed beta pdf model is used. The presumed beta pdf shape is not flexible enough to describe the singly conditional pdfs of a reacting scalar undergoing extinction/reignition. However, the strong nonlinearity of the chemical source term can cancel the deviations under a singly conditional presumed beta pdf shape closure strategy, equation (6) in this paper. The insensitivity of the model to the conditional variance of the reacting scalar suggests the possibility of using the conditional variance which results from the fluctuations of the dissipation rate of the mixture fraction alone.

Acknowledgments

This paper was presented at the 18th International Colloquium on the Dynamics of Explosions and Reactive Systems (Seattle, Washington, August 2001).

The authors express gratitude to Paiboon Sripakagorn for making available to us his DNS database before publication. Funding by the US Department of Energy within the ASCI program is also gratefully acknowledged.

References

Bilger R W 1980 Turbulent flows with nonpremixed reactants *Turbulent Reacting Flows (Topics in Applied Physics no 44)* (Berlin: Springer) chapter 3, pp 65–113

Cha C M, Kosály G and Pitsch H 2001 Modeling extinction and reignition in turbulent nonpremixed combustion using a doubly-conditional moment closure approach *Phys. Fluids* **13** 3824–34

Klimenko A Y and Bilger R W 1999 Conditional moment closure for turbulent combustion *Prog. Energy Combust. Sci.* **25** 595–687

Kronenburg A, Bilger R W and Kent J H 1998 Second-order conditional moment closure for turbulent jet diffusion flames *Proc. Combust. Inst.* **27** 1097–104

Mastorakos E and Bilger R W 1998 Second-order conditional moment closure for the autoignition of turbulent flows *Phys. Fluids* **10** 1246–8

Peters N 1983 Local quenching due to flame stretch in non-premixed turbulent combustion *Combust. Sci. Tech.* **30** 1–17

Pitsch H, Cha C M and Fedotov S Flamelet modeling of non-premixed turbulent combustion with moderate local extinction and re-ignition *Combust. Theory Modelling* submitted

Pitsch H and Fedotov S 2001 Investigation of scalar dissipation rate fluctuations in non-premixed turbulent combustion using a stochastic approach *Combust. Theory Modelling* **5** 41–57

Press W H, Teukolsky S A, Vetterling W T and Flannery B P 1992 *Numerical Recipes in FORTRAN* 2nd edn (Cambridge: Cambridge University Press)

Ross S 1984 *A First Course in Probability* 2nd edn (London: Macmillan)

Sripakagorn P, Kosály G and Pitsch H 2000 Local extinction–reignition in turbulent nonpremixed combustion *CTR Annual Research Briefs* Stanford University/NASA Ames, pp 117–128

Swaminathan N and Bilger R W 1998 Conditional variance equation and its analysis *Proc. Combust. Inst.* **27** 1191–8